ACS OMEGA

Article

Cite This: ACS Omega 2018, 3, 7243−7246

Quantitative Investigation for the Dielectrophoretic Effect of Fluorescent Dyes at Single-Cell Resolution

Yagmur Yildizhan,[†] Umut B. Gogebakan,[†] Alara Altay,[†] Monsur Islam,[‡] Rodrigo Martinez-Duarte,[‡] and Meltem Elitas*[,†]

[†]Faculty of Engineering and Natural Sciences, Sabanci University, Istanbul 34956, Turkey

[‡]Mechanical Engineering Department, Clemson University, Clemson, South Carolina 29634-0921, United States

Supporting Information

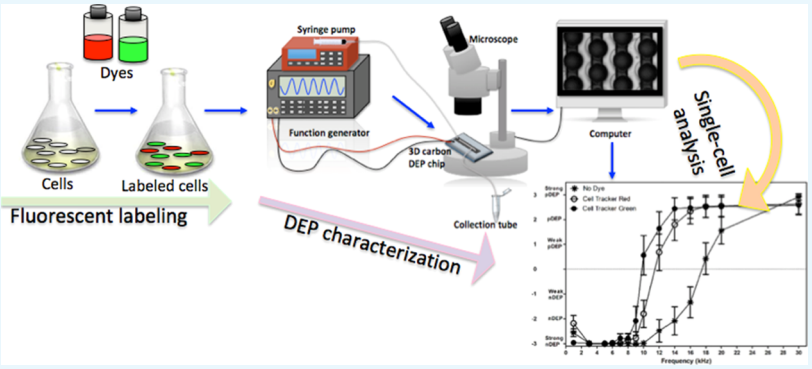

ABSTRACT: Most of the microscopy-based, quantitative assays rely on fluorescent dyes. In this study, we investigated the impact of fluorescent dyes on the dielectrophoretic response of the mammalian cells. The dielectrophoretic measurements were performed to quantify whether the fluorescent dyes alter the dielectrophoretic properties of the cells at single-cell resolution. Our results present that when 10 V_{pp} electric field is applied, the fluorescent-labeled cells experienced the crossover frequency at 8−10 kHz, whereas the label-free cells exhibited at 16−18 kHz.

1. INTRODUCTION

In the late 19th century, the discovery of organic fluorescent compounds provided an avenue for capturing the dynamic processes of living organisms. Various fluorescent dyes have been developed. They have become essential tools for powerful techniques ranging from live-cell fluorescence imaging to flow cytometry, with various applications including the detection of substances, the tracking of single molecules, and the visualization of post-translational modifications.[1−7] Although label-free assays that exclude phenotypic and genetic modifications might be more suitable for many life sciences and medical applications, fluorescent dyes remain one of the most valuable tools for current state-of-the-art assays and technologies. Various fluorescent dyes have been developed with improved sensitivity, selectivity, specificity, detection speed, repeatability, photostability, brightness, and biocompatibility.[1,2,8,9] Modern biotechnological tools in conjunction with these better-quality fluorescent dyes will play a significant role in understanding cellular and subcellular dynamics in the near future as well.

This study presents the dielectrophoretic behavior of pre- and postlabeled single cells when stained with commercially available fluorescent dyes. Dielectrophoresis (DEP) is one of the label-free characterization methods that directly and quantitatively determine whether or not fluorescent dyes alter the intrinsic properties of the cells. Herbert Pohl introduced the DEP phenomenon in the 1950s as the motion of an electrically polarizable particle in a nonuniform electric field.[10,11] The dielectrophoretic force depends on the permittivity of the suspending medium of the cells (ε_m), the radius of the cell (r), the real part of the Clausius−Mossotti factor (f_{CM}), and the applied electric field (E), as represented in eq 1.

$$F_{DEP} = 2\pi\varepsilon_m \, \mathrm{Re}[f_{CM}]\nabla {E_{rms}}^2 \quad (1)$$

The Clausius−Mossotti factor is defined as in eq 2, where ε_c^* is the complex permittivity of the cell, and ε_m^* is the complex permittivity of the medium.

$$\mathrm{Re}[f_{CM}] = \frac{\varepsilon_c^* - \varepsilon_m^*}{\varepsilon_c^* + 2\varepsilon_m^*} \quad (2)$$

The complex permittivity (ε^*) depends on permittivity (ε), conductivity (σ) of the cell/medium, and frequency (f) of the electric field (E), as expressed in eq 3, where j shows the imaginary number $\sqrt{-1}$.

Received: March 21, 2018
Accepted: June 20, 2018
Published: July 3, 2018

DOI: 10.1021/acsomega.8b00541
ACS Omega 2018, 3, 7243−7246

$$\varepsilon^* = \varepsilon - \frac{j\sigma}{2\pi f} \quad (3)$$

When $\mathrm{Re}[f_{CM}] > 0$, the strong electric field regions attract the cells, and they are influenced by "positive DEP (pDEP)"; when the cells are repelled from the high field strength, they are designated "negative DEP (nDEP)". Both the pDEP and nDEP behavior of the cells rely on their polarizability difference with respect to their surrounding medium. When the polarizability difference between the cells and their surrounding medium is almost negligible, the DEP forces become very weak, to almost zero. This specific frequency is known as "crossover frequency", which determines the dielectrophoretic characteristics of the cells.[12−15]

Since the 1950s, many new DEP tools and methods with improved sensitivity, throughput, and practical usage have been developed.[16−20] Here, we used the three-dimensional (3D) carbon-electrode DEP, which was introduced by Dr. Martinez-Duarte and his colleagues. It has been previously used in a variety of cell separation applications including bacteria, yeast, and mammalian cells.[13−15,21]

In this study, we investigated the dielectrophoretic effect of two different commercially available membrane-permeant reactive tracer dyes (The CellTracker Green CMFDA (5-chloromethyl fluorescein diacetate) and CellTracker Red CMTPX (Fisher Scientific) on U937, the (pro-) monocytic, human myeloid leukemia cell line (ATCC CRL 1593.2). As these two dyes are well-suited and widely studied not only for being easy to use but also adequate for monitoring the behavior of cells, cell location or movement, and long-term cell tracking thanks to retaining in the living cells through several generations. Besides, multiplexing green and red fluorescent dyes allows the observation of cell−cell communication and protein expressions without cross-contamination. Although these dyes were studied for their cytotoxicity, stability, and other chemical properties, according to our knowledge, investigation on the dielectrophoretic properties of these commercially available fluorescent cell tracker dyes have not been performed yet.[22,23]

2. RESULTS AND DISCUSSION

U937 cells were cultured in an RPMI (Rosewell Park Memorial Institute, Sigma-Aldrich) medium supplemented with 10% fetal bovine serum (Sigma-Aldrich) and 1% Pen/Strep (penicillin−streptomycin, Sigma-Aldrich) in 75 cm^2 flasks (Corning T-75 flasks) in an incubator (NUVE EC160), in which 37 °C, 5% CO_2, and humidity were maintained. The CellTracker Green CMFDA and CellTracker Red CMTPX dyes were used to prepare a 1 μM staining solution in fresh RPMI medium. Complementing the fluorescent dyes into the medium did not change the conductivity of the medium. The number of U937 monocyte cells was adjusted to 1×10^5 cells/mL using a hemocytometer (Marienfeld). Next, the cells were cultured in the staining solution in the incubator for 30 min. Then, the stained cells were harvested at 3000 rpm (Hettich EBA 20 centrifuge) for 5 min to remove any residual dye in the culture media. Afterward, the cells were resuspended in a low-conductive DEP buffer twice. The DEP buffer was prepared using 8.6% sucrose (BioFroxx), 0.3% glucose (Sigma-Aldrich), and 0.1% bovine serum albumin (PAN Biotech) in deionized (DI) water. The conductivity of the DEP buffer was measured as 20 μS/cm using a conductivity meter (Corning, 311 conductivity).

The dielectrophoretic setup consists of a function generator, an upright, optical microscope integrated with a camera, a computer, a syringe pump, and the 3D carbon-DEP device. There are two 20−200 μL pipette tips at the inlet and outlet of the electrode-array microchannel to create reservoirs. The Tygon tubing connects the syringe and the microchannel in the system.

The dielectrophoretic characterization of label-free and stained U937 monocyte cells was performed using the experimental setup illustrated in Figure 1. First, the 3D carbon-DEP chip was sterilized by flowing 70% ethanol and then DI water prior to the experiments. Next, the bubbles inside the microchannel were removed and the chip was filled with the low-conductive DEP buffer. The cells were prepared as explained above and introduced into the chip with a 10 μL/min flow rate using the syringe pump (New Era Pump Systems, Inc., NE-1000). When the cells reached the region of the carbon electrodes, the flow was stopped. The cells were settled when a signal with 10 V_{pp} at frequencies between 1 kHz and 20 MHz was applied from the function generator (INSTEK—GFG-8216A). After the DEP exposure, the cells were collected from the device into a collection tube for further inspection. A Nikon Eclipse, an upright optical microscope with 10× objective, was used to capture videos with 1 frame/s frame rate during the experiments (Figure 2).

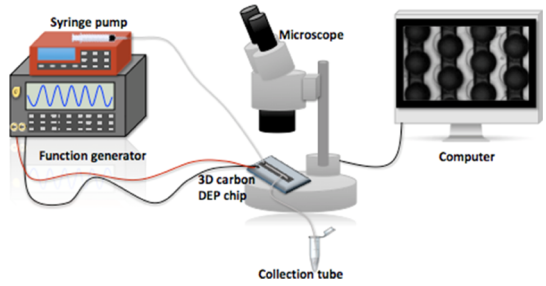

Figure 1. Illustration of the experimental setup.

The obtained videos were analyzed as demonstrated in Figure 3 and detailed in the previous studies of Dr. Martinez-Duarte and co-workers.[24−26] The location of the cells at each frame was rated as strong nDEP (−3), nDEP (−2), weak nDEP (−1), crossover (0), weak pDEP (1), pDEP (2), or

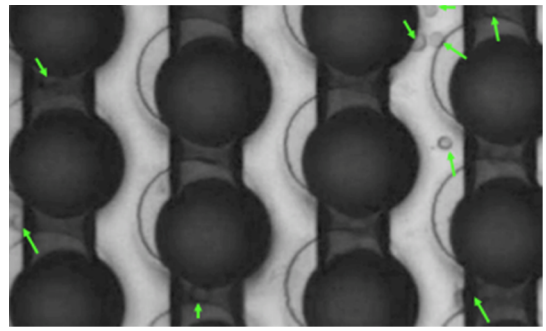

Figure 2. Image of the label-free U937 cells in the 3D carbon electrode array. Green arrows show the cells, black circles are the carbon electrodes, and black lines are the connection wires of the electrodes.

DOI: 10.1021/acsomega.8b00541
ACS Omega 2018, 3, 7243−7246

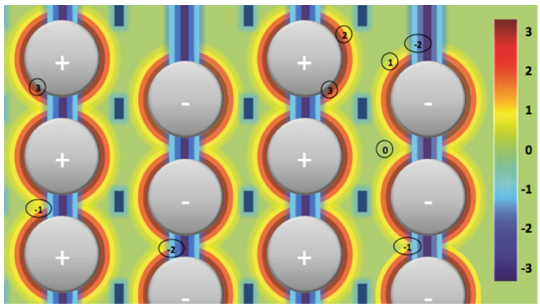

Figure 3. Schematic diagram for the image analysis on the 3D carbon-electrode microchip that represents the DEP regions, according to the captured image in Figure 2.

strong pDEP (3) according to their positions with respect to the carbon electrodes.

Figures 4 and 5 show the obtained dielectrophoretic behavior of the label-free U937 monocytes. The monocytes

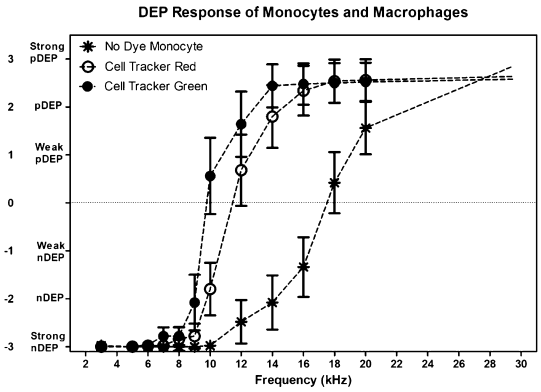

Figure 4. DEP response of monocytes stained with CellTracker Red (white circles), CellTracker Green (black circles), and DEP response of unlabeled monocytes (star). A total of 50 cells were tracked from 1 to 30 kHz at 10 V_{pp}.

were stained with CellTracker Red and CellTracker Green dyes. To delineate whether the applied fluorescent dyes affect the DEP characteristics of the cells, dielectrophoretic forces were applied between 1 kHz and 20 MHz at 10 V_{pp} in the 3D carbon-DEP chip. As there was no drag force because of the fluid flow in the system, the translational movement of the cells was due to the exhibited DEP forces (eq 1). Next, the location of the cells was correlated with their DEP responses. The position of each cell was traced in each frame using the obtained movies (Supporting Movie). ImageJ was used to analyze the captured images. The mean value of the positions of the cells with standard deviations at each frequency was calculated using the Prism software (GraphPad).

3. CONCLUSIONS

Fluorescent dyes have been widely used as tremendous tools for cell labeling in a wide variety of applications of life sciences and medicine, such as monitoring chemotaxis and invasion, tracking cell movement and migration, and quantifying proliferation. They are easy to use and compatible with several assays. Their fluorescent signal is retained in living cells through several generations. For these dyes, most of the conventional characterization assays and methods quantify their sensitivity, selectivity, brightness, photostability, specific-

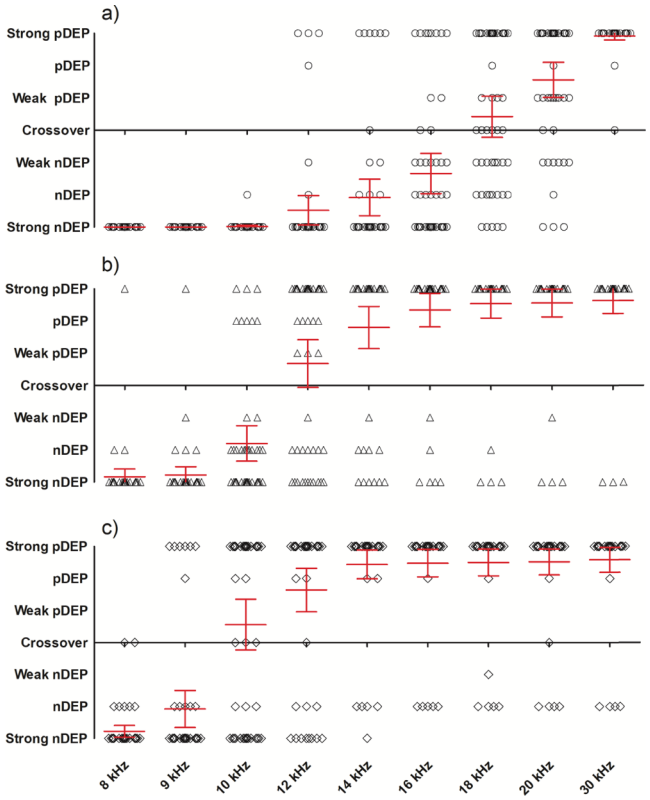

Figure 5. DEP responses of monocytes at single-cell resolution. (a) Unlabeled monocytes, (b) monocytes stained with CellTracker Red, (c) monocytes stained with CellTracker Green. Fifty cells were tracked for each frequency from 1 to 30 kHz at 10 V_{pp}. The red lines show the mean and standard deviation for the cells at each frequency.

ity, toxicity, and photochemical properties. As most of the fluorescent dyes are capable of penetrating through the cell membrane, passing into the cytoplasm, and being impermeant, we investigated whether the fluorescent dyes change the permittivity and conductivity of the cells that may influence the dielectric properties of the cells. To the best of our knowledge, this is the first study that investigates the dielectrophoretic properties of commercially available fluorescent cell tracker dyes. As shown in Figures 4 and 5, there is a slight shift in the crossover frequencies of the cells when they are labeled with membrane-permeant reactive tracers. This minor variation might be negligible for many applications; nevertheless, it might be significant for the dielectrophoretic separation of cells that exhibit very close dielectrophoretic responses at single-cell resolution.

■ ASSOCIATED CONTENT

Supporting Information

The Supporting Information is available free of charge on the ACS Publications website at DOI: 10.1021/acsomega.8b00541.

Characterization movie showing the dielectrophoretic behavior of single cells with/without fluorescent dyes when 10 V_{pp} is applied between 1 and 30 kHz (ZIP)

■ AUTHOR INFORMATION

Corresponding Author

*E-mail: melitas@sabanciuniv.edu (M.E.).

DOI: 10.1021/acsomega.8b00541
ACS Omega 2018, 3, 7243−7246

ORCID

Meltem Elitas: 0000-0001-6502-6314

Notes

The authors declare no competing financial interest.

■ ACKNOWLEDGMENTS

The authors gratefully acknowledge the support from the Faculty of Engineering and Natural Science at Sabanci University and Sabanci University Nanotechnology Research and Application Center (SUNUM).

■ REFERENCES

(1) Hayashi-Takanaka, Y.; Stasevich, T. J.; Kurumizaka, H.; Nozaki, N.; Kimura, H. Evaluation of chemical fluorescent dyes as a protein conjugation partner for live cell imaging. *PLoS One* **2014**, *9*, e106271.

(2) Fei, X.; Gu, Y. Progress in modifications and applications of fluorescent dye probe. *Prog. Nat. Sci.* **2009**, *19*, 1−7.

(3) Nienhaus, K.; Ulrich Nienhaus, G. Fluorescent proteins for live-cell imaging with super-resolution. *Chem. Soc. Rev.* **2014**, *43*, 1088−1106.

(4) Jung, D.; Min, K.; Jung, J.; Jang, W.; Kwon, Y. Chemical biology-based approaches on fluorescent labeling of proteins in live cells. *Mol. BioSyst.* **2013**, *9*, 862−872.

(5) van de Linde, S.; Heilemann, M.; Sauer, M. Live-cell super-resolution imaging with synthetic fluorophores. *Annu. Rev. Phys. Chem.* **2012**, *63*, 519−540.

(6) Haugland, R. P. Spectra of Fluorescent Dyes Used in Flow Cytometry. *Methods in Cell Biology*; Academic Press, 1994; Vol. *42*, Chapter 37, pp 641−663.

(7) Kennedy, M. D.; Jallad, K. N.; Thompson, D. H.; Ben-Amotz, D.; Low, P. S. Optical imaging of metastatic tumors using a folate-targeted fluorescent probe. *J. Biomed. Opt.* **2003**, *8*, 636−641.

(8) Terai, T.; Nagano, T. Small-molecule fluorophores and fluorescent probes for bioimaging. *Pfluegers Arch.* **2013**, *465*, 347−359.

(9) Dsouza, R. N.; Pischel, U.; Nau, W. M. Fluorescent dyes and their supramolecular host/guest complexes with macrocycles in aqueous solution. *Chem. Rev.* **2011**, *111*, 7941−7980.

(10) Pethig, R. Review-Where Is Dielectrophoresis (DEP) Going? *J. Electrochem. Soc.* **2017**, *164*, B3049−B3055.

(11) Pohl, H. A. The motion and precipitation of suspensoids in divergent electric fields. *J. Appl. Phys.* **1951**, *22*, 869−871.

(12) Hughes, M. P. Fifty years of dielectrophoretic cell separation technology. *Biomicrofluidics* **2016**, *10*, 032801.

(13) Elitas, M.; Martinez-Duarte, R.; Dhar, N.; McKinney, J. D.; Renaud, P. Dielectrophoresis-based purification of antibiotic-treated bacterial subpopulations. *Lab Chip* **2014**, *14*, 1850−1857.

(14) Yildizhan, Y.; Erdem, N.; Islam, M.; Martinez-Duarte, R.; Elitas, M. Dielectrophoretic Separation of Live and Dead Monocytes Using 3D Carbon-Electrodes. *Sensors* **2017**, *17*, 2691.

(15) Martinez-Duarte, R.; Renaud, P.; Madou, M. J. A novel approach to dielectrophoresis using carbon electrodes. *Electrophoresis* **2011**, *32*, 2385−2392.

(16) Nakano, A.; Ros, A. Protein dielectrophoresis: advances, challenges, and applications. *Electrophoresis* **2013**, *34*, 1085−1096.

(17) Li, M.; Li, W. H.; Zhang, J.; Alici, G.; Wen, W. A review of microfabrication techniques and dielectrophoretic microdevices for particle manipulation and separation. *J. Phys. D: Appl. Phys.* **2014**, *47*, 063001.

(18) Bakewell, D. J.; Bailey, J.; Holmes, D. Real-time dielectrophoretic signaling and image quantification methods for evaluating electrokinetic properties of nanoparticles. *Electrophoresis* **2015**, *36*, 1443−1450.

(19) Hu, X.; Bessette, P. H.; Qian, J.; Meinhart, C. D.; Daugherty, P. S.; Soh, H. T. Marker-specific sorting of rare cells using dielectrophoresis. *Proc. Natl. Acad. Sci. U.S.A.* **2005**, *102*, 15757−15761.

(20) Faraghat, S. A.; Hoettges, K. F.; Steinbach, M. K.; van der Veen, D. R.; Brackenbury, W. J.; Henslee, E. A.; Labeed, F. H.; Hughes, M. P. High-throughput, low-loss, low-cost, and label-free cell separation using electrophysiology-activated cell enrichment. *Proc. Natl. Acad. Sci. U.S.A.* **2017**, *114*, 4591−4596.

(21) Islam, M.; Natu, R.; Larraga-Martinez, M. F.; Martinez-Duarte, R. Enrichment of diluted cell populations from large sample volumes using 3D carbon-electrode dielectrophoresis. *Biomicrofluidics* **2016**, *10*, 033107.

(22) Zhou, W.; Kang, H. C.; O'Grady, M.; Chambers, K. M.; Dubbels, B.; Melquist, P.; Gee, K. R. CellTrace Far Red & CellTracker Deep Red—long term live cell tracking for flow cytometry and fluorescence microscopy. *J. Biol. Methods* **2016**, *3*, e38.

(23) Bernhard, J. M.; Ostermann, D. R.; Williams, D. S.; Blanks, J. K. Comparison of two methods to identify live benthic foraminifera: A test between Rose Bengal and CellTracker Green with implications for stable isotope paleoreconstructions. *Paleoceanography* **2006**, *21*, PA4210.

(24) Martinez-Duarte, R.; Camacho-Alanis, F.; Renaud, P.; Ros, A. Dielectrophoresis of lambda-DNA using 3D carbon electrodes. *Electrophoresis* **2013**, *34*, 1113−1122.

(25) Martinez-Duarte, R. Carbon-electrode Dielectrophoresis for Bioparticle Manipulation. *ECS Trans.* **2014**, *61*, 11−22.

(26) Natu, R.; Martinez-Duarte, R. Numerical Model of Streaming DEP for Stem Cell Sorting. *Micromachines* **2016**, *7*, 217.

DOI: 10.1021/acsomega.8b00541
ACS Omega 2018, 3, 7243−7246